AUSTRALIAN JOURNAL OF BASIC AND APPLIED SCIENCES

ISSN:1991-8178 EISSN: 2309-8414
Journal home page: www.ajbasweb.com

Surfactant- Coated Magnetite Nanoparticles as Superior Adsorbent for Rapid Removal of the of Reactive Orange 4 from Wastewaters

Hilal Nora M., Ahmed.H.M, Emam. A.G., ELsisi, A.A.

Chemistry Department, Faculty of Science, Al-Azhar University (Girls), Nasr City, Cairo, Egypt.

Address For Correspondence:
Hilal Nora M., Chemistry Department, Faculty of Science, Al-Azhar University (Girls)
E-mail: profdrnorahilal@azhar.edu.eg, norahelal832@yahoo.com

ARTICLE INFO

Article history:
Received 18 June 2017
Accepted 28 July 2017
Available online 20 August 2017

Keywords:
Nanoparticles Magnetite (NPs-MG) Coated Nanoparticles Magnetite (NPs-CMG) Reactive Azo Dye Cetyltrimethylammonium Bromide(CTAB) Adsorption Kinetic Isotherm Thermodynamic Parameters

ABSTRACT

The object of this study was to evaluate the efficiency of the Reactive Orange 4(RO4) dye removal with application of magnetite nanoparticles (NPs-MG) and modified with Cetyltrimethylammonium bromide (NPs-CMG) were used as an adsorbent. The characteristics of the magnetite nanoparticles (NPs-MG) were studied using Fourier transform infrared (FTIR), scanning electron microscopy (SEM), EDX analysis and X-ray diffraction (XRD). Batch adsorption experiments were performed as a function of initial dye concentration, contact time, solution pH, temperature and adsorbent dosage on dye removal. The adsorption kinetic and adsorption isotherms of the reactive orange 4 (RO4) onto adsorbents was discussed using various models. The experimental data fitted well for pseudo second order model. Freundlich model is more appropriate to explain the nature of adsorption with high correlation r^2 coefficient. Thermodynamic parameters like the Gibbs free energy (ΔG^o), enthalpy (ΔH^o), and entropy (ΔS^o) were also determined and they showed that the adsorption process was feasible, spontaneous, and endothermic in the temperature range of 297–328° K. The obtained results in the present study indicated that Cetyltrimethylammonium bromide (CTAB) coated Fe_3O_4 NPs can be an efficient adsorbent material for removal of reactive orange 4 (RO4) from aqueous solutions.

INTRODUCTION

Over the last few decades, society has become increasingly sensitive towards the protection of the environment. Considering that dyes are, by definition, highly visible materials, even minor releases into the environment may cause the appearance of color. In addition to this, many dyes are toxic and/or mutagenic to aquatic life (Venceslau,1994). The total amount of dye consumption by the textile industries worldwide is approximately one million kilograms of dyes are discharged per year into our waters and streams by the textile industries (Orfao, 2006). A wide range of physical and chemical processes such as flocculation, electro-flotation, precipitation, electro-kinetic coagulation, ion exchange, membrane filtration, oxidation, irradiation and ozonation have been investigated extensively for removing dyes from aquatic bodies (Golder,2005 and Lazaridis, 2003). However, these processes are costly and cannot effectively be used to treat the wide range of wastewater containing dyes (Tarley, 2004). Two most available technologies for dye removal are oxidation and adsorption. Oxidation methods are possibly the best technologies to totally eliminate organic carbons, but they are only effective for wastewaters with very low concentrations of organic compounds (Sun,1997). Adsorption has been found to be superior to other techniques for removal of colors, odor, oils, and organic pollutants from process or waste effluents due to its initial cost, simplicity of design and ease of operation (Juang., 2002). Textile effluents

To Cite This Article: Hilal Nora M., Ahmed.H.M, Emam. A.G., ELsisi, A.A., Surfactant- Coated Magnetite Nanoparticles as Superior Adsorbent for Rapid Removal of the of Reactive Orange 4 from Wastewaters. ***Aust. J. Basic & Appl. Sci.,*** *11(11): 194-204, 2017*

are known toxicants, which inflict acute disorders in aquatic organism's uptake of textile effluents through food chain in aquatic organisms may cause various physiological disorders like hypertension, sporadic fever, renal damage, cramps etc. Reactive Orange 4 is one such effluent which causes various disorders when present in aqueous solution. Hence the treatment of wastewater containing dye is a challenging problem (Kaviyarasan, 2006). Consequently, substantial amounts of unfixed dyes which are then released into the wastewaters display high organic loads. Recently, magnetic separation has been applied in many areas to remove, isolate and/or concentrate the desired components from a sample solution. Nano sized magnetic iron oxide particles have been studied extensively as a new adsorbent with large surface area and small diffusion resistance (Liao,2002) for the separation and removal of chemical species such as metals, dyes and gases (Faraji,2010). To enhancement the ability of magnetic nanoparticles surface for removal of pollutant was modified using several materials such as surfactants. The surface properties of nanoparticles can be modified with a surfactant. This is favored by van der Waals interaction between surfactant and the adsorbent. In general, surface modification can be accomplished by physical and/or chemical adsorption of the desired molecules to coat the surface, depending on the specific applications (Mahmoodi, 2015).

The present work aims to study an appropriate and economic procedure for removal of the reactive orange 4 (RO4) from water by adsorption on the NPs of Fe_3O_4 (NPs-MG) and coated - CTAB (NPs-CMG) as a magnetic adsorbent. The dye adsorption isotherm, kinetic and effect of operational parameters such as, contact time, solution pH and adsorbent dosage, temperature and initial dye concentration was evaluated in detail.

Experimental:

Chemical:

All reagents were of analytical reagent grade and were used as supplied. the reactive orange 4 (RO4) was obtained from Ciba-Gigy (Germany) and used without further purification. The characteristics of dyes were shown in Table 1. Ferric chloride $FeCl_3$. $6H_2O$), ferrous chloride ($FeCl_2.4H_2O$), sodium hydroxide, and hydrochloric acid were purchased with high purity from Merck (Darmstadt, Germany). A stock standard solution of (RO4) dye at a concentration of 1000 mg/L was prepared in doubly distilled water. This standard solution was diluted with distilled water to prepare solutions with concentration of 10 to 150 mg /L of dye. These solutions were used for optimization of effective parameters and also, for plotting the calibration curve in order to calculate the dye removal efficiency with spectrophotometric technique. Solutions of 1 M of sodium hydroxide (NaOH) and 1M HCl were used to adjust the pH.

Table 1: Characteristics of Reactive Orange 4

Chemical Name	Reactive Orange 4
CAS Registry number	12225-82-0
Specification	Molecular Formula : $C_{24}H_{16}C_{l2}N_6O_{10}S_3$ Molecular Weight : 781.47gm
C.I. No.	18260
λ max	= 488 nm
Structure	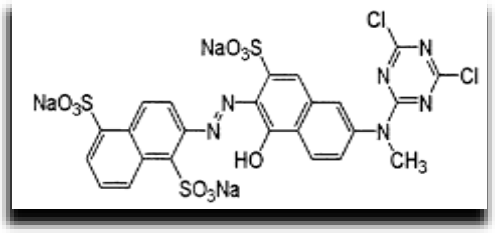

Synthesis of Fe_3O_4 NPs:

NPs -Fe_3O_4 (NPs-MG) were prepared by a chemical co-precipitation method using a reactor which was designed in our previous work (Takafuji,2004) without using any surfactant. The Fe_3O_4 NPs synthesized were characterized using a scanning electron microscope (SEM), infrared radiation (IR) and X-ray diffraction (XRD).

Adsorption of reactive azo dye:

Optimization studies were carried out according to the following procedure:

40mL aqueous solutions of the dye (75 mg/ l) , 0.1 gm of the Fe_3O_4 NPs was added to the dye solutions, pH of the solutions were adjusted to the desired value and Cetyltrimethylammonium bromide (CTAB) was added into the dye solutions as percentages then the mixture solutions were stirred for 15 min. After dye adsorption; NPs-MG were quickly separated from the sample solutions using a magnet (1.4 T), and the residual dye concentrations

in the supernatant clear solutions were determined spectrophotometrically using a calibration curve. The following equation was applied to calculate the dye removal efficiency in the treatment experiments:

$$\% \text{ Removal} = \frac{C_o - C_e}{C_o} \text{ x } 100 \quad (1)$$

The equilibrium sorption capacity of the NPs-magnetite and coated magnetite by CTAB at a given time was determined by using the mass balance equation:

$$q_e = (C_o - C_e)\frac{V}{W} \quad (2)$$

where C_o and C_e are the initial and residual concentrations of the dye in the solution (mg /l), respectively, v is the volume of the solution, and w is the mass of adsorbent (mg) and q_e is the adsorption capacity of the NPs-MG at equilibrium (mg/g).

RESUITS AND DISCUSSIONS

Characterizations of NPs-MG :

FT-IR Analysis:

The FT-IR spectra were recorded to prove the successful preparation of NPs-MG and possible interaction between various constituents of nanoparticles and CTAB surfactant. FT-IR spectrum of the NPs-MG and coated nanoparticles magnetite NPs-CMG are shown in (Fig.1a), The peak at ~ 3455 cm^{-1} is attributed to the stretching vibrations of ─OH, which is assigned to surface OH groups of NPs-MG. The peak at ~ 571 cm^{-1} is attributed to the Fe─O band vibration of Fe_3O_4. Also, the peak at ~ 1380 cm^{-1} is attributed to C─N band and the peaks at 2885 and 2925 cm-1 are attributed to two different C─H bands vibration of CTAB. The IR spectra show that Fe_3O_4 NPs surface was well modified by CTAB.

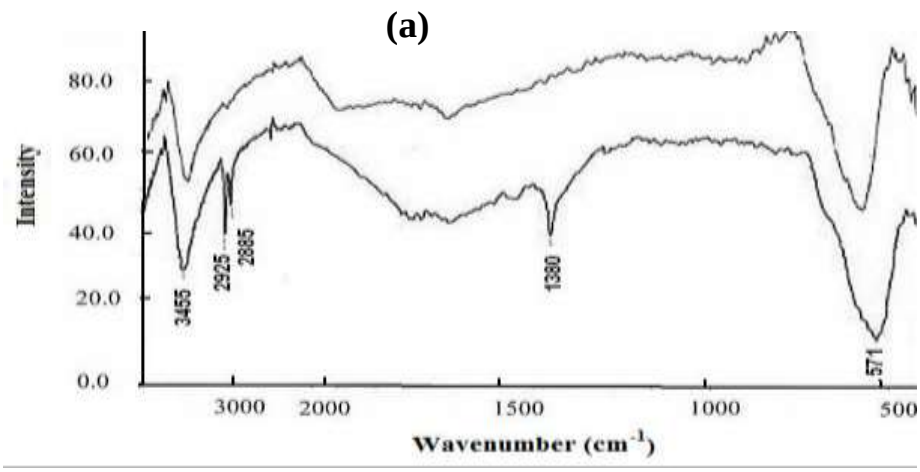

XRD Analysis:

The crystal structure of NPs-MG was characterized using XRD for 2θ diffraction angles from 20° to 60°. As shown in (Fig.1b), the sharp peaks at 30.124°, 35.476°, 43.135°, 53.506°, and 56.991° in the XRD pattern are matches well with the reported standard pattern (JCPDSNo.75-1372). The diffraction peaks are quite sharp and no peaks for impurities are detected. The results show the sample is nano-Fe_3O_4 which has high purity and well-crystallizes structure.

(b)

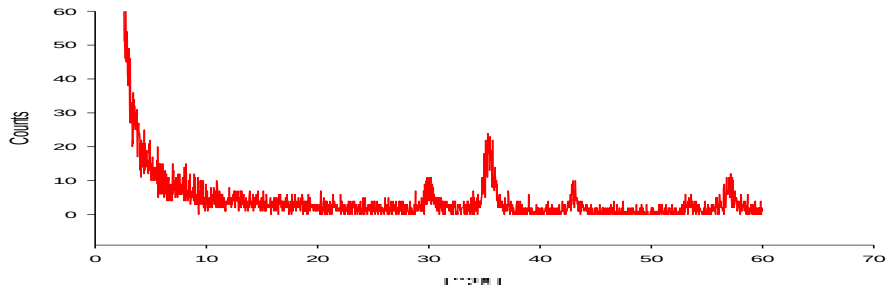

SEM and EDX:

SEM image was a quested to determine the morphology and particle size of the adsorbent NPs-MG (Fig. 1c) where the nanoparticles were obtained to be spherical and of average size of 20 nm with narrow size distribution. The EDX analysis (Fig. 1d), shows that the nanoparticles consist of Fe and O elements. Results from Table 2 confirms the appearance of Fe_3O_4 nanoparticles.

(c)

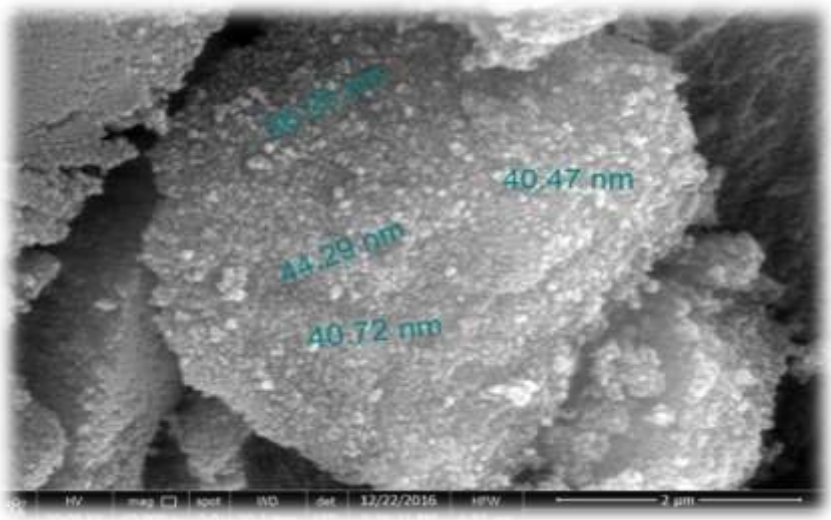

(d)

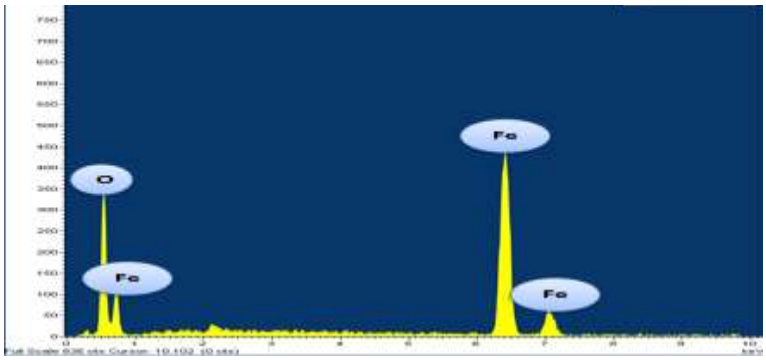

Fig. 1: Characterization of the NPs-MG: **(a)** The IR spectra of NPs-MG and NPs-CMG**(b)** The XRD pattern of the NPs-MG, **(c)** The SEM image of the NPs-MG**(d)** EDX mapping of the NPs-MG

Table 2: Persentage of elements in Fe_3O_4 nanoparticles

Element	Weight%	Atomic%
C K	7.16	15.07
O K	38.69	61.11
Fe K	52.02	61.11
Au M	2.12	0.27

Adsorption Studies:

Effect of pH:

The pH of the system exerts profound influence on the adsorptive uptake of the dye presumably due to its influence on the surface properties of the adsorbent and ionization/dissociation of the dye. The degree of adsorption of these ions onto the adsorbent surface is primarily influenced by the surface charge on the adsorbent, which in turn is influenced by solution's pH. In the acidic range 1 – 3, the positive surface charge of adsorbent increases and this would attract the negatively charged functional groups on the reactive dyes. When the pH is increased, the number of negatively charged sites increases and there will be competition between the negatively charged hydroxyl ions and anionic dye for the sorption sites and the adsorption rate get decreased (Baseri,2012). For NPs-MG, the surface charge is neutral at pH_{zpc}, which is about 7.0 (Faraji,2010). Based on the results (Fig. 2), pH significantly affect RO4 adsorption efficiency, it was found that the maximum adsorption efficiency of RO4 was obtained in an acidic solution. In the acidic pH·s, NPs-MG, the dye are in anionic form (due to sulfites groups) and can interact with the positively charged surface of NPs-MG. On the other hand, at alkaline pH, surface

of NPs-MG is negatively charged and the dyes are negative too. So, the dyes can't directly interact with NPs-MG surface. But in the presence of CTAB, its molecules interact with the negatively charged surface of NPs-MG and create a positive surface at a pH =8.0 ±0.5 via coating of the surface of NPs-Fe_3O_4 (Fig. 2) and then the dyes can interact. So the maximum adsorption efficiency of RO4 onto NPs-CMG (96.44%) is achieved at pH =8.0±0.5

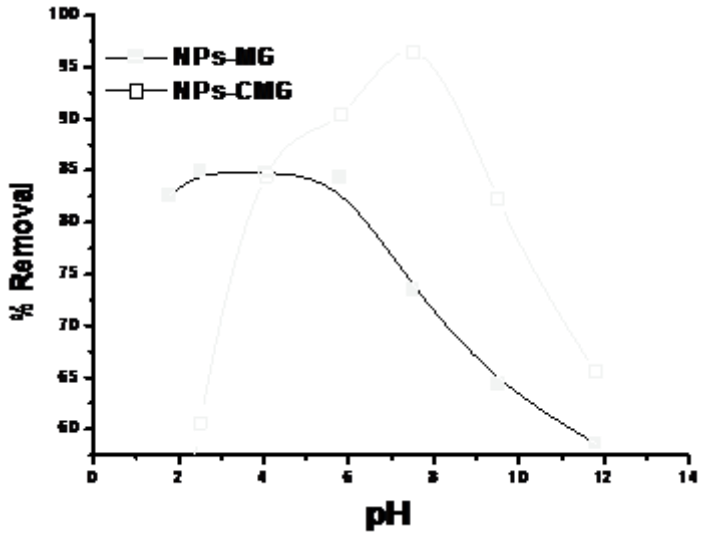

Fig. 2: Effect of pH on removal percentage (0.10 g of adsorbent in 75 mg/l of RO4, and, 24°C).

Effect of adsorbent dosage:

The dye removal using NPs-MG and NPs-CMG ([RO4]: 75 mg/l,24ºC and pH = 2.5±0.5 of NPs-MG and 8.0±0.5 of NPs-CMG) at different adsorbent dosages (g) was shown in Fig. 3.The increase in dye removal with adsorbent dosage is due to the increasing of adsorbent surface and availability of more adsorption sites. However, if the removal percentage of material decreased with the increasing amount of adsorbent, it can be attributed to overlapping or aggregation of adsorption sites resulting in a decrease in total adsorbent surface area available to the dye and an increase in diffusion path length (Crini,2008). The highest percentage of dye removal was attained with an adsorbent dose of 0.1 g.

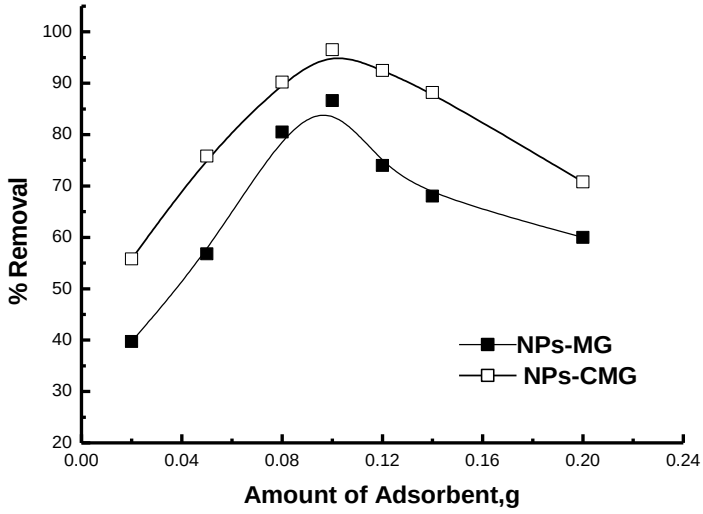

Fig. 3: Effect of adsorbent dosage on removal percentage. (75 mg/l, 24ºC and pH = 2.5±0.5 of NPs-MG and 8.0±0.5 of NPs-CMG)

Effect the Percentage Concentrations of Surfactant on Adsorption of the Dye:

CTAB plays an important role in the dye adsorption mechanism. Fig. 4 depicts the adsorption capacity of RO4 as a function of the CTAB amount added**.** According to the results, in alkaline conditions like pH = 8.0±0.5 the dyes are adsorbed via CTAB on the surface of NPs- MG. Therefore, at alkaline pH, is found with increasing amounts of CTAB, the adsorption efficiency will increase. On the other hand, at high percentage concentrations

of CTAB, the adsorption capacity (q_e, mg/g) decreased due to the formation of CTAB (micelles and/or) ion-pairing between dyes and excess amounts of CTAB which reduce the interaction of negative dyes with positively charged surface of NPs- MG**.** The optimum amount of CTAB was found to be 0.08%.

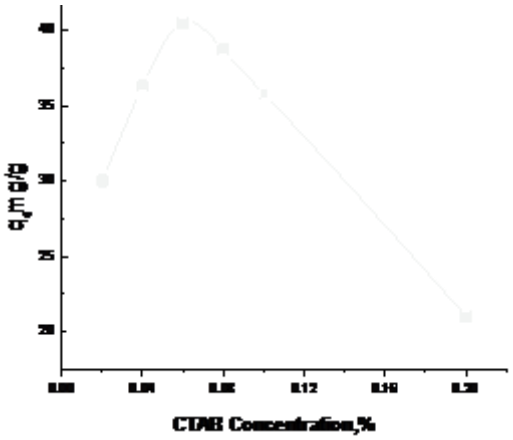

Fig. 4: Effect of CTAB concentration on adsorption capacity (75 mg/l, 24^{o}C and 8.0±0.5 of NPs-CMG)

Effect of Contact Time:

As the time of adsorption is changed from 3 to 150 minutes, adsorption capacity firstly increased, and afterwards no change is observed. As time progresses the surface coverage of the adsorbent is high, and further no adsorption takes place. Fig. 5 shows the effect of time on adsorption capacity. According to these results, the agitation time was fixed at 1 hour for the rest of the batch experiments to make sure that equilibrium was attained, which is considered adequate and economical for wastewater treatment (Kadirvelu,2003).

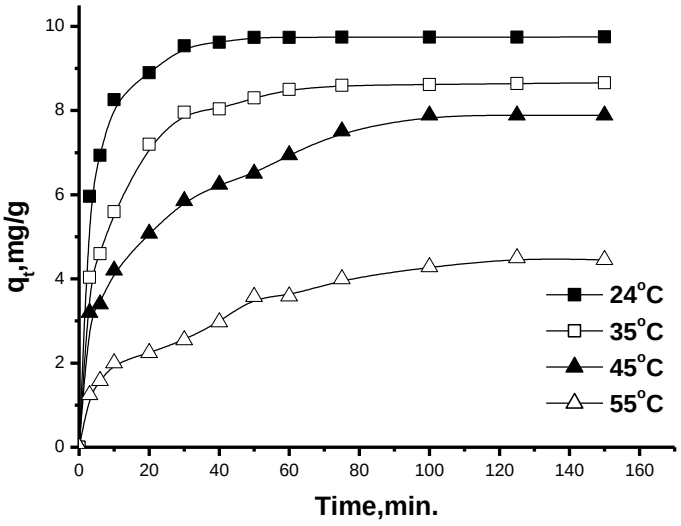

Fig. 5: Effect of contact time on the adsorption capacity ($q_e$mg/g) of RO4 on NPs-MG at different temperatures. ([dye] = 75 mg/l. pH = 2.5 ± 0.5 and adsorpent dose = 0.1g)

Adsorption Kinetics:

Kinetic parameters, which are helpful for the prediction of the adsorption rate, give important information for designing and modeling the adsorption processes. Kinetic studies were performed in a 1.0 L glass beaker, where 0.1g of NPs-MG, were added into 50 ml of the dye solution (75 mg /l) with at ambient temperature (24^{o}C). The removal rate of RO4 was very fast during the initial stages of the adsorption processes. However, the equilibrium adsorption times were reached about 75 min for at 75 mg/ l dye concentration. The kinetic data for adsorption of the dye were analyzed using pseudo-first order (Lagergren,1998), pseudo-second order (Chien,1980), intra-particle diffusion models and Liquid film diffusion model (Sakthivel,2013) to find out the adsorption rate expression. The conformity between experimental data and the model-predicted values was expressed by the correlation coefficients (r^2, values close to 1).

Pseudo-first order and pseudo-second order models:

The pseudo-first-order equation can be expressed as in the following equation:

$$\log (q_e - q_t) = \log q_e - \frac{k_1}{2.303} t \quad (5)$$

Linear form of pseudo-second order model

$$\frac{t}{q_t} = \frac{1}{k_2 q_e^2} + \frac{t}{q_e} \quad (6)$$

where, q_e and qt are the amount of dye adsorbed (mg/ g) at equilibrium and time, t (min); k_1 is the rate constant of pseudo-first order (min^{-1}); k_2 is the rate constant of pseudo second- order (g/mg /min) for adsorption.The parameters $k_1$and $q_e$could be calculated from the slope and the intercept of the plots of log $(q_e - q_t)$ versus t, and are found to be unbeseeming for the present system. This suggests that the pseudo-first-order kinetic model is not suitable to describe the adsorption process. The q_e and $k_2$values can be obtained from the slope and the intercept of plots of t/q_t versus t, which are illustrated in Fig. 6 and are listed in Table 3 for adsorption of RO4 on NPs-MG and NPs-CMG respectively. The calculated correlation coefficients (r^2) (close to 1) of the pseudo-second order kinetic model were higher than those of the pseudo-first-order kinetic model; this indicated that the pseudo-second-order model fitted the experimental data better (Patil,2015).

Sum of Error Squares:

The percentage of sum of error squares is given as (Inbaraj,2002),

$$SE\ (\%) = \sqrt{\Sigma[(q_e)_{exp} - (q_e)_{cal}]^2 / N} \quad (7)$$

where N is the number of data points, $(q_e)_{exp}$ is the experimental q_e, $(q_e)_{cal}$ is the calculated q_e. The values were calculated and are presented in Table 3. It shows that $(q_e)_{cal}$ of second order kinetics is close to $(q_e)_{exp}$. It can be seen that SE (%) value is lower for the pseudo second order kinetic model. This confirms the applicability of the pseudo second order kinetic model. The correlation coefficient (r^2) for pseudo first order model ranged between 0.760 and 0.823 whereas these values for the second order model were close to 1. Based on the values of regression coefficient, the second order kinetic model was more suitable to describe the adsorption process of using dye adsorption (RO4) than a pseudo first order model.

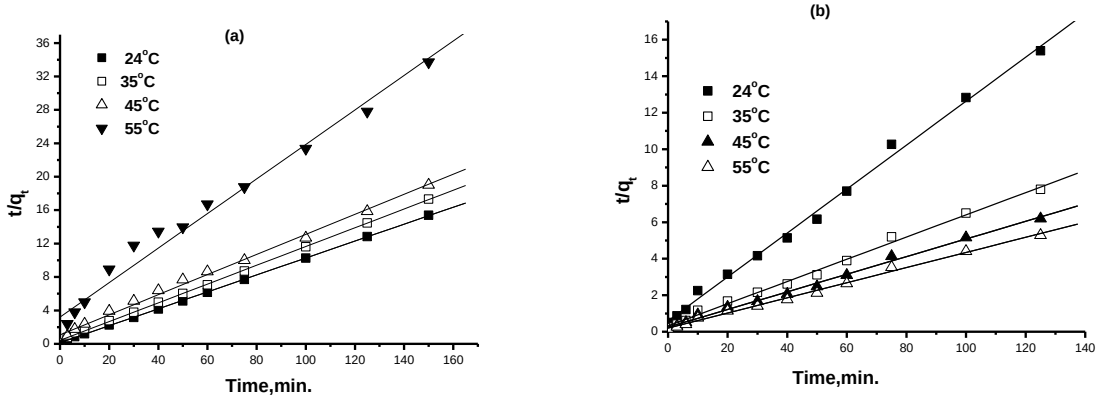

Fig. 6: Fitting of the kinetic data to the pseudo-second order kinetic model of RO 4 on (a) NPs-MG and (b) on NPs-CMG at different temperatures. (pH = 2.5±. [dye] = 75 mg/l and adsorbent dose = 0.1g)

Table 3: Comparison of the pseudo second-order adsorption rate constants for NPs-MG and NPs-CMG

Temp. °C	Pseudo-Second Order Model of NPS-MG					Pseudo-Second Order Model of NPS-CMG				
	q_e calc., mg/g	q_e exp. mg/g	k_2x10^2 g/mg/min	r^2	SE (%)	$q_e$calc.,mg/g	q_e exp. mg/g	k_2x10^3 g/mg/min	r^2	SE (%)
24	9.87	10.01	1.32	0.999	0.044	24.11	28.36	8.73	0.998	1.34
35	8.91	9.6	1.40	0.999	0.218	20.70	24.23	9.31	0.999	1.12
45	8.21	8.51	3.01	0.999	0.095	16.42	19.12	11.70	0.996	0.854
55	4.84	4.95	7.43	0.989	0.098	8.31	9.74	24.4	0.999	0.452

Intraparticle diffusion and Liquid film diffusion models:

The time dependent data from this study was further used to investigate whether intra-particle and liquid film diffusion kinetics also played significant roles in the adsorption of RO4 ions from their aqueous solutions. The

intra-particle diffusion kinetic plots of q_t against $t^{1/2}$ for RO4 was taken and presented in Fig 7 . To investigate if intra-particle diffusion was the sorption rate limiting step, the Weber-Moris plot of qt versus $t^{1/2}$ was taken equation:

$$q_t = k_{id} t^{1/2} + C \quad (8)$$

where k_{id} is the intra-particle diffusion rate constant (mg/g $min^{1/2}$) and C (mg/ g) is a constant that gives an idea about the thickness of the boundary layer; it was observed that the larger the value of C the greater the boundary layer effect (Weber Jr,1963). Comparing the k_{id1} values for the macropore and micropore diffusion stages for RO4 ions show that the rate limiting step is the micropore diffusion stage. This is because the micropore diffusion constant k_{id2} value for RO4 ions was lower than those for the macropore diffusion constants k_{id1}. This shows that the rate of micropore diffusion is the slower step and the rate determining step. The boundary layer effect i.e. the intercepts of the second lines from the plots in Fig.7 was also presented in Table 4, which further shows greater effect at the micropore diffusion stage than at the macropore stage at different temperatures.Liquid film diffusion model (Hameed,2008) was also used in this study to investigate if transport of dye from the liquid phase up to the solid phase boundary also plays a role in the adsorption process equation:

$$\ln (1 - F) = -kfdt \quad (9)$$

where F is the fractional attainment of equilibrium ($F = q_t/q_e$), k_{fd} is liquid film diffusion constant. A linear plot of ─ ln (1─F) versus t with zero intercept would suggest that the kinetics of the sorption process was controlled by diffusion through the liquid surrounding the solid sorbent. q_e is the adsorption capacity of the sorbent at equilibrium (mg/ g). Adsorption is a multilayer process, involving transport of solute particle from the aqueous phase to the surface of the solid adsorbent followed by diffusion into the interior of the pores. The liquid film diffusion model obtained from the slopes and intercepts of 8 and their regression coefficients (r^2) are presented in Table 4. The intercept values at different temperatures are higher than zero, but are close to the origin showing the significance of liquid film diffusion in the rate determination of the adsorption process. The regression coefficient (r^2) values were relatively high showing the relevance of film diffusion as a rate determining factor in the adsorption process.

Table 4: Intra-particle and liquid film diffusion constants and regression coefficients (r^2) for RO4 on NPs-MG at different temperatures.

	Intraparticle diffusion Model						Liquid Film Diffusion Model		
Temp.°C	k_{id1}	C_1	r_1^2	k_{id2}	C_2	r_2^2	k_{fd}	Intercept	r^2
24	0.975	4.492	0.997	0.002	9.730	0.934	0.033	1.508	0.871
35	0.909	2.631	0.974	0.030	8.303	0.908	0.033	0.694	0.906
45	0.590	2.231	0.981	0.016	6.063	0.890	0.041	-0.173	0.905
55	0.282	0.881	0.979	0.013	2.952	0.980	0.033	-0.0245	0.914

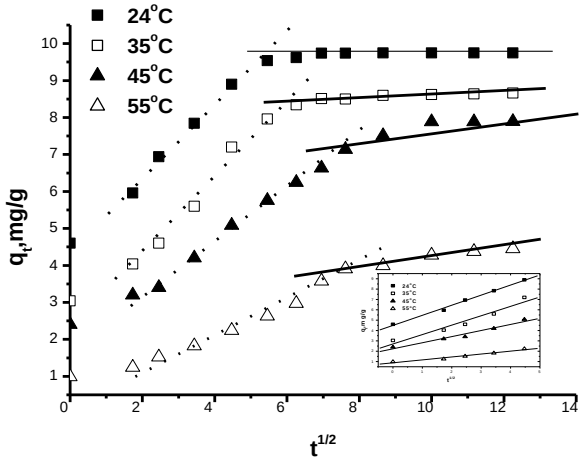

Fig. 7: Intraparticle diffusion model of RO4 dye with adsorbent (NPs-MG) at different temperatures. (pH = 2.5 ± 0.5. [dye] = 75 mg/l. adsorbent dose = 0.1g).

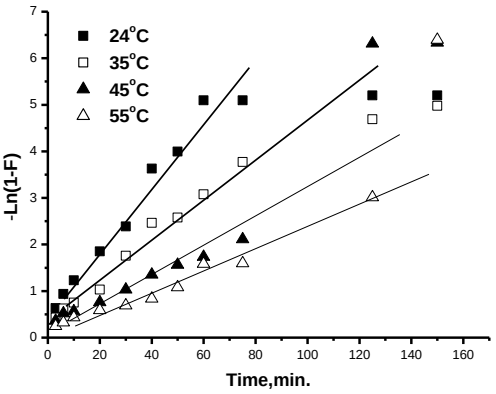

Fig. 8: Liquid film diffusion model of RO4 dye with adsorbent (NPs-MG) at different temperatures. (pH $= 2.5 \pm 0.5$. [dye] $= 75$ mg/l. adsorbent dose $= 0.1$g).

Adsorption isotherm:

The equilibrium adsorption isotherms are one of the most important figures that help to understand the mechanism of adsorption and describe how adsorbates could interact with adsorbents. The current research presents a method of direct comparison of the isotherm fit of several models to enable the best-fit and best isotherm parameters to be obtained. Several isotherms such as Langmuir, Freundlich and Temkin models were studied in details (Zeng, 2014, Zhou, 2014 and Mittal, 2013).

Langmuir model:

The linear form of Langmuir equation can be written as follows:

$$\frac{C_e}{q_e} = \frac{C_e}{q_m} + \frac{1}{K_L q_m} \tag{10}$$

where C_e (mg/l) is the concentration of RO4 at equilibrium, q_e (mg/g) is the amount of RO4 adsorbed by the NPs-MG at equilibrium, q_m (mg/g) is the maximum adsorption capacity corresponding to monolayer coverage, and k_L (l/mg) is the Langmuir constant. The values of $q_m$and $k_L$can be calculated from plotting C_e/q_eversus C_e. In order to determine if the adsorption process is favorable or unfavorable, a dimensionless constant, separation factor or equilibrium parameter R_L, is defined according to the following equation.

$$R_L = \frac{1}{1 + k_L C_o} \tag{11}$$

where k_L (l/mg) is the Langmuir constant and C_o (mg/l) is the initial RO4 concentration. The $R_L$value indicates adsorption process is irreversible when $R_L$is 0; favorable when $R_L$is between 0 and 1; linear when $R_L$is 1; and unfavorable when $R_L$is greater than 1 (Mahmoudi,2014).The Langmuir plots for RO4 adsorption on NPs-MG are obtained in Fig.9, and the parameters are shown in Table 5. The values of the correlation coefficient for the Langmuir plots changed in the range 0.990-0.992.

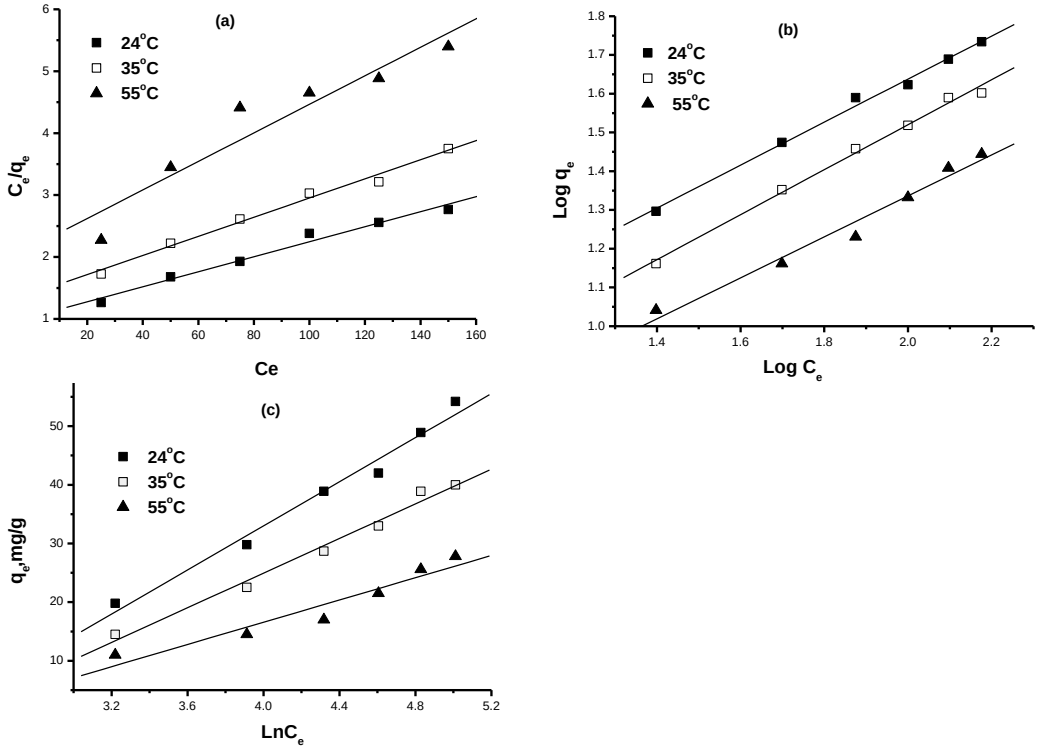

Fig. 9: Fitting of isotherm data to(a) the Langmuir model, (b) the Freundlich modeland(c) the Temkin model of RO4 on NPs-MG at different temperatures. ($\mathrm{pH} = 2.5 \pm 0.5, [\mathrm{dye}] = 75\ \mathrm{mg/l}, \mathrm{adsorbent\ dose} = 0.1\mathrm{g}$)

Freundlich model:

The linear form of Freundlich equation is given as:

$$\log q_e = \log k_F + \frac{1}{n}\log C_e \quad (12)$$

where q_e is the RO4 concentration on NPs-MG at equilibrium, C_e (mg/l) is the concentration of RO4 in solution at equilibrium, and k_F and 1/n are Freundlich constants related to adsorption capacity and adsorption intensity, respectively (Padmavathy,2016). Freundlich constants are calculated from the slope and the intercept in Fig 9, and are given in Table 5. The correlation coefficients (r^2> 0.0.9999) reflect that the experimental data agree well with the Freundlich model. The values of 1/n are all smaller than 1, so they represent the favorable adsorption conditions.

Tempkin isotherm:

Temkin and Pyzhev (Temkin,1940 and Elwakeel,2009) considered the effect of the adsorbate interaction on adsorption and proposed the model known as the Temkin isotherm, which can be expressed as:

$$qe = (RT/\beta)\, lnA + (RT/\beta)\, \ln Ce \quad (13)$$

where A and B are Temkin constant, R is the gas constant and T is the absolute temperature. A Plot of q_e versus $\ln C_e$ can be used to determine the constant A and B, where $B=(RT/\beta)$. The Temkin adsorption isotherm model was chosen to evaluate the adsorption potentials of the adsorbent for adsorbates. The Temkin isotherm plot for RO4 is presented in Fig. 9 and Table 5. The Temkin isotherm considered the effects of indirect the heat of adsorption of all the adsorbate molecules on the adsorbent surface layer would decrease linearly with coverage due to adsorbate –adsorbate interactions.

Table 5: Isotherm Parameters for Adsorption of RO4 onto NPs-MG.

Temp.°C	Langmuir isotherm				Freundlich isotherm			Tempkin isotherm		
	q_{max}	k_L	R_L	r^2	1/n	k_f	r^2	A	B	r^2
24	82.65	0.012	0.526	0.990	0.555	3.373	0.997	0.106	18.80	0.990
35	64.52	0.011	0.548	0.994	0.580	2.286	0.996	0.099	14.76	0.993
45	43.48	0.010	0.557	0.990	0.529	1.898	0.998	0.105	9.48	0.961

Adsorption Thermodynamics:

The thermodynamics of adsorption can be investigated by the values of K_c at different temperatures according to the following van't Hoff equation (Mittal,2013)

$$\ln Kc = \frac{\Delta S^\circ}{R} - \frac{\Delta H^\circ}{R\,T} \quad (14)$$

where K_c is the equilibrium constant, (q_e/C_e) is the adsorption distribution coefficient, (ΔH^o) is the standard enthalpy change (kJ /mol), (ΔS^o) is standard entropy change (kJ/ mol. K), T is the temperature in Kelvin and R is the universal gas constant (8.314 J/ mol. K). Plotting ln K_c against 1/T (Fig. 10) gives a straight line with slope and intercept equal to $\Delta H°$/R and $\Delta S°$/R, respectively .The calculated values of thermodynamic parameters are shown in Table 6. The positive value of ΔH^o confirms the endothermic character of dye sorption, whereas the positive ΔS^o value confirms a certain increased randomness at the solid-solute interface during sorption. Gibbs free energy of the adsorption ($\Delta G°$) can be calculated from the following equation and given in Table 6. The negative value of $\Delta G°$ shows spontaneity of adsorption process.

$$\Delta G° = \Delta H° - T\Delta S° \quad (15)$$

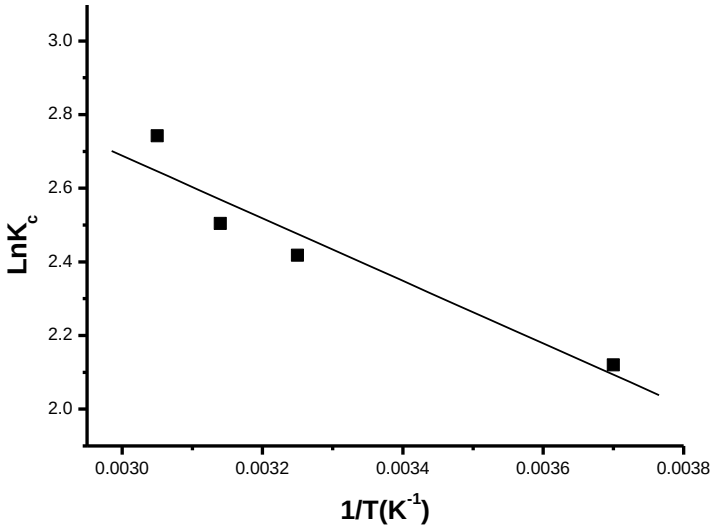

Fig. 10: The van't Hoff plot of RO4 on NPs-MG at different temperatures. ($pH = 2.5 \pm .$ [dye] = 75 mg/l and adsorbent dose = 0.1g)

Table 6: Thermodynamic Parameters of RO4 on NPs-MG.

Temp.^{o}K	$\Delta G°$(kJ /mol)	$\Delta H°$ (kJ /mol)	$\Delta S°$ (J /mol.K)
297	-5.87	7.066	43.55
308	-6.13		
318	-6.78		
328	-7.22		

Activation Energy:

The rate constant k_2 at different temperatures listed in Table 3 was used to estimate the activation energy of the RO4 adsorption onto NPs-MG and coated magnetite NPs-CMG. Assume that the correlation among the rate constant, k_2, temperature, T and activation energy, Ea, follows the Arrhenius equation, which induces the following expression:

$$\ln k2 = -\,Ea/R\,(1/T) + const \quad (16)$$

where R is the gas constant, the slope of plot of lnk_2 versus 1/T was used to evaluate Ea. The value of Ea was estimated to be 17.24 kJ/mol, 9.53 kJ/mol for NPs-MG and NPs-CMG respectively. The magnitude of activation energy gives an idea about the type of adsorption. The physisorption usually have energies in the range 5-40 kJ/mol, while higher activation energies of 40-800 kJ/mol suggest chemisorptions. The activation energy < 40 kJ/mol for the dye indicates the diffusion controlled physisorption. Similar results are also reported for the adsorption of Lanaset Grey G on activated carbon (Nollet,2003). The activation energy of diffusion of RO4 onto

NPs-MG (17.24 kJ/mol) is significantly higher than that of RO4 onto NPS-CMG (9.53 kJ/mol). This means that the activation energy of diffusion of RO4 is lowered by 47.06 % for NPs-CMG adsorbent.

Conclusions:

This study investigated the equilibrium and the dynamics the adsorption of an anionic dye, which is namely Reactive Orange 4 (RO4) dye onto nanoparticles magnetite (NPs-MG) and coated with Cetyltrimethylammonium bromide (NPs-CMG) were used as an adsorbent. The effects of major variables governing the efficiency of the process such as, contact time, adsorbent dose, surfactant concentration, initial dye concentration and pH to saturate the available sites located on (NPs-MG) and (NPs-CMG) surface. The adsorption followed the pseudo-second order kinetic model. There was significant evidence to show that liquid film diffusion was also a rate determining step in the adsorption process. The adsorption equilibrium data were fitted to Freundlich isotherm rather than Langmuir and Temkin isotherm. The results indicated the applicability of the method for removal of anionic dyes from aqueous solutions. The activation energy of diffusion of RO4 onto NPs-MG is significantly higher than that of RO4 onto NPs-CMG. The adsorption of the Reactive Orange 4dye at various temperatures shows that the adsorption is spontaneous, endothermic and marked with an increased randomness at the solid–liquid interface. This study may provide a guideline for efficient removal of other dyes from dye-containing effluents by using coated magnetic nanoparticles in alkaline medium. Due to very high surface areas, short diffusion route and magnetically-assisted separability of the CTAB-coated Fe_3O_4NPs high adsorption capacities can obtain in a very short time.

REFERENCES

Ai, L., Y. Zeng, J. Jiang, 2014. Hierarchical porous BiOI architectures: facilemicrowave nonaqueous synthesis, characterization and application inthe removal of Congo red from aqueous solution, J .Chem Eng., 235: 331-339.

Baseri, J.R., P.N. Palant, P. Sivakumar, 2012. adsorption of reactive dye by anoval activated carbon prepared from thevetia, Inter. J. of Chem. Research, 3(2): 36-41.

Chien, S.H., W.R. Clayton,1980. Application of Elovich equation to the kinetics of phosphate release and sorption on soils, Soil Sci. Soc. Am. J. 44: 265-268.

Crini, G., F. Gimbert, C. Robert, B. Martel, O. Adam, N. Morin-Crini, F. De Giorgi, P.M. Badot, 2008. The removal of basic blue 3 from aqueous solutions by chitosan-basedadsorbent: batch studies. J Hazard Mater, 153(1): 96-106.

Elwakeel, K.Z., 2009. J Hazard Mater, 167: 383-389.

Faraji, M., Y. Yamini, M. Rezaee, 2010. Extraction of trace amounts of mercury with sodium dodecyle sulphate-coated magnetite nanoparticles and its determination by flow injection inductively coupled plasma-optical emission spectrometry, Talanta, 81: 831-836.

Faraji, M., Y. Yamini, A. Saleh, M. Rezaee, M. Ghambarian, R. Hassani, 2010. A nanoparticle-based solid-phase extraction procedure followed by flow injection inductively coupled plasma-optical emission spectrometry to determine some heavy metal ions in water samples, Anal. Chim. Acta, 659: 172-177.

Faraji, M., Y. Yamini, E. Tahmasebi, A. Saleh, F. Nourmohammadian, 2010. Cetyltrimethyl ammoniumbromide-coated magnetite nanoparticles as highly efficientadsorbent for rapid removal of reactive dyes from the textile companies wastewaters, J. Iran. Chem. Soc., 7: 130-144.

Golder, A.K., N. Hridaya, A.N. Samanta, S. Ray, 2005. Electrocoagulation of methylene blue and eosin yellowish using mild steel electrodes J. Hazard. Mater., 127: 134-140.

Hameed, B.H., I.A.W. Tan, A.L. Ahmad, 2008. Adsorptionisotherm, kinetic modeling and mechanism of 2,4,6-trichlorophenol on coconut husk-based activated carbon, J .Chem Eng., 144(2): 235-244.

Inbaraj, S., N. Sulochana, 2002. Indian J Chem Technol., 9: 201-208.

Juang, R.S., F.C. Wu, R.L. Tseng, 2002. Characterization and use of activated carbons prepared from bagasse for liquid-phase adsorption, Colloids Surf., A 201: 191-199.

Kadirvelu, K., C. Namasivayam, 2003. Activated carbon from coconutcoirpith as metal adsorbent: adsorption of Cd (II) from aqueous solution, Adv. Environ. Res., 7: 471-478.

Karthikeyan, S., M. Jambulingam, P. Sivakumar, A.P. Shekhar and J. Krithika, 2006. E-J Chem., 3(4): 303-306.

Lazaridis, N.K., T.D. Darapantsios, D. Georgantas, 2003. Kinetic analysis for the removal of a reactive dye from aqueous solution onto hydrotalcite by adsorption, Water Res., 37: 3023-3033.

Lagergren, S., Handlingar, 1998. 24: 1-39.

Liao, M.H., D.H. Chen, 2002. Fast and efficient adsorption/desorption of protein by a novel magnetic nano-adsorbent ,Biotechnol. Lett., 24: 1913-1917.

Mahmoodi, N.M., 2015. Surface modification of magnetic nanoparticle and dye removal from ternary systems, J. Indust. and Engin.Chem, 27: 251-259.

Mahmoudi, Z., S. Azizian, B. Lorestani, 2014. Removal of methylene blue from aqueous solution: A comparison between adsorption by iron oxidenanospheres and ultrasonic degradation, J. Mater. Environ. Sci., 5: 1332-1335.

Manohar R. Patil, V.S. Shrivastava, 2015. Adsorptionremoval of carcinogenic acid violet19 dye from aqueous solution by polyaniline-Fe_2O_3 magnetic nano-composite, J.Mater. Environ.Sci., 6(1): 11-21.

Mittal, A., D. Jhare, J. Mittal, 2013. Adsorption of hazardous dye Eosin Yellow from aqueous solution onto waste material De-oiled Soya: Isotherm, kineticsand bulk removal. J Mol Liquids, 179: 133-140.

Nollet, H., M. Roels, P. Lutgen, 2003. Meeran D&Verstraete,Chemosphere, 53: 655-671.

Orfao, J.J.M., A.I.M. Silva, J.C.V. Pereira, S.A. Barata, I.M. Fonseca, P.C.C. Faria, M.F.R. Pereira, 2006. J. Colloid Interface Sci., 296: 480-489.

Padmavathy, K.S.A., G. Madhub, P.V. Haseena, 2016. A study on effects of pH, adsorbent dosage, time, initial concentration and adsorption isotherm study for the removal of hexavalent chromium (Cr (VI)) from wastewater by magnetite nanoparticles Procedia Technol., 24: 585-594.

Sakthivel, K., I. Arockiaraj, C. Kannan, S. Karthikeyan, 2013. Film- Pore diffusion Modeling for Sorption of Azo Dye on to Oneand Three Dimensional Nano Structured Carbon Nano Materialsfrom Jatropha Curcas, J. Environ. Nanotechnol., 2: 66.

Sun, G., X. Xu, Ind. Eng., 1997. Sunflower stalks as adsorbents for color removal from textile wastewater Chem. Res., 36: 808-881.

Tarley, C.R.T., M.A.Z. Arruda, 2004. Biosorption of heavy metals using rice milling byproducts: characterisation and application for removal of metals from aqueous effluents, Chemosphere, 54: 987-995.

Takafuji, M., S. Ide, H. Ihara, Z. Xu, 2004. Preparation of poly(1-vinylimidazole)-graftedmagnetic nanoparticles and their application for removal of metal ions Chem.Mater., 16: 1977-1983.

Temkin, M.I., V. Pyzhev, 1940. Kinetics of ammoniasynthesis on promoted iron catalysis, Acta, Phsicochim, USSR, 12: 217-221.

Venceslau, M.C., S. Tom, J.J. Simon, 1994. Characterisation of textile wastewaters-a 453 review. Environ.Technol,. 15: 917-929.

Weber, W.J., J.C. Morris, 1963. Kinetics of adsorption on carbon from solution, Journal of Sanitary Engineering Division,ASCE, J.Sanitary Engin. Division,ASCE,. 89: 31-59.

Zhou, L., J. Huang, B. He, F. Zhang, H. Li, 2014. Peach gum for efficient removal of methylene blue and methyl violet dyes from aqueous solution, Carbohydr Polym, 101: 574-581.